

# Using Embedded Electrical Grid for Active Thermography Diagnostics of Composite Structures

---

A. ORŁOWSKA, J. BICZYK and P. KOŁAKOWSKI

## ABSTRACT

Thermovision techniques, which are generally used in manufacturing industry for process control, were for a long time limited by low measurement sensitivity and poor possibilities of fast, high frequency data acquisition. As soon as these problems were overcome, thermovision cameras became a valuable tool for damage diagnostics.

Thermovision based structural health monitoring techniques dedicated for composite structures are widely discussed by many researchers. The most popular approaches are: pulse-heating thermography, lock-in thermography, vibro-thermography and step-heating thermography. All these methods use external excitation in the form of thermal or mechanical vibration sources.

The thermal source used in the proposed method is a 3D electrical grid, embedded in the structure and composed of through-the-layer and surface-layer elements. The diagnostics are based on the fact that a small current applied to the grid generates a scattered thermal field corresponding to the grid layout. Loss of the adhesion between layers in a particular area is accompanied by simultaneous break of the grid conductors in that area. Consequently, the thermal field density in the damaged zone will be decreased. The effect of a forced temperature field is experimentally observed by a long-wave thermovision camera.

---

Anita Orłowska, Jan Biczuk, Przemysław Kołakowski, Adaptronica sp. z o. o., R&D company, Szpitalna 32, 05-092 Łomianki, Poland, email: [aorlow@adaptronica.pl](mailto:aorlow@adaptronica.pl), <http://www.adaptronica.pl>

Anita Orłowska, Smart-Tech Centre, Institute of Fundamental Technological Research, Pawińskiego 5B, 02-106 Warsaw, Poland, <http://smart.ippt.gov.pl>

## INTRODUCTION

Thermovision techniques, which are generally used in manufacturing industry for process control, were for a long time limited by low measurement sensitivity and poor possibilities of fast (high frequency) data acquisition. As soon as these problems were overcome, thermovision cameras became a valuable tool for damage diagnostics at quite affordable prices. Experimental thermoelastic analysis of the stress state in structures was developed in the mid 1980s in the form of stress pattern analysis by a thermal emission (SPATE) system [5], using sensitive infrared detectors to measure small changes in temperature. The advent of thermovision enabled a come-back of this methodology with new sensitivity ranges.

Intensification of research based on thermal field observation was a natural consequence. The most popular thermovision techniques are:

- pulse-heating thermography (PHT)—where thermal excitation sources are applied in the impulse mode and measurements are collected during the self-cooling phase of the sample,
- lock-in thermography (LIT)—where thermal excitation is harmonic, and amplitude variations and phase shifts in relation to the excitation signal are analyzed,
- step-heating thermography (SHT)—where excitation sources are laser impulses which interact with the sample locally (the thermal conductivity is determined in this method on the basis of the thermal field rate),
- vibro-thermography (VT)—where vibration-inducing excitation (most often by sonic or ultrasonic waves) reveals a perturbation of thermal waves due to defects.

Most of thermovision methods require a huge amount of energy and homogeneous heating of the examined structure. In case of complex structural elements, homogeneous heating of a large area using traditional techniques, i.e. exterior sources of heat such as lamps or heaters, is a difficult task. An alternative solution could be the use of methods based on mechanical excitation of ultrasonic frequencies or elaboration of a new group of materials, with the so-called additional functionality, i.e. possessing the ability of partial self-diagnosis. A proposition of such material was presented in [6].

The technique proposed in this paper uses a specially designed 3D electrical grid, embedded in the structure and composed of through-the-layer and surface-layer elements, as shown in Fig. 1a. The loss of the adhesion between layers in a particular area is accompanied by simultaneous break of the grid conductors in that area. Consequently, the thermal field density in the delamination zone will be decreased. The effect of a forced temperature field is experimentally observed by a long-wave thermovision camera. The temperature range is a few degrees above the temperature of the environment. Because of the assumption of simultaneous failure of the composite and the embedded electrical circuit, the area of delamination was modeled in numerical simulations as a wire-free region, which was identified by lower temperatures when the thermal excitation was applied. The corresponding experimental result is depicted in Fig. 1d.

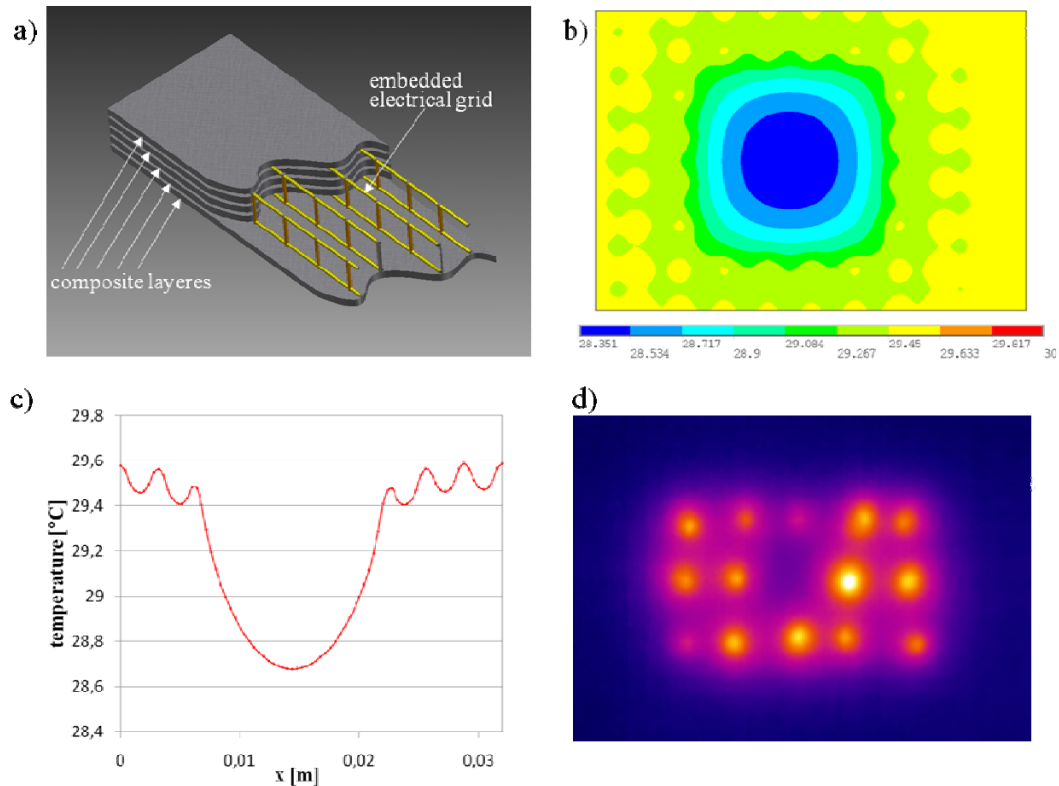


Figure 1. Electrical grid embedded in composite material for SHM purposes a) in-plane temperature distribution for delaminated composite specimen – numerical simulation results for static load b) cross-sectional temperature distribution along the line going through the center of the delamination area c) thermogram captured for a real composite specimen with one conductive element broken d) cf. [6].

In particular cases, the proposed method can be a good alternative for methods using exterior sources of thermal energy or mechanical excitation. It seems that the ability to detect damages in elements of relatively big thickness and the ease of interpretation of results are significant advantages of the presented method.

Most of doubts are related with the problem of adding the third material component to the smart composite (except for fibers and resin) which is the embedded electrical grid supposed to provide the heat excitation. It is a challenge to embed the grid in the matrix in a way which guarantees the assumed mechanical and thermo-mechanical interactions.

In this paper, the authors consider the influence of the temperature field generated by the embedded electrical grid on structural response of the composite. Comparison of stress fields caused by the temperature load in some composites of different thermoelastic properties, i.e. based on glass and carbon fibers, is presented. To increase the calculation speed, an elementary volume of the examined material corresponding to a slice of the composite containing four internal sources of heat, has been considered (Fig. 2).

## THERMAL-STRUCTURAL ANALYSIS

Because of the fact that the coupling between the temperature field and the deformation field is weak, a sequential method can be applied for the thermal-structural analysis for the stationary problem of the thermal-structural analysis.

In the sequential analysis, the two fields are coupled by using results from the thermal analysis as an input for the stress analysis. In this paper, the nodal temperatures obtained from the thermal analysis are used as input loads for the stress analysis.

The Laplace equation for stationary heat transfer yields:

$$\nabla^2 T = 0 \quad (1)$$

where  $\nabla$  is the Hamilton operator,  $T$  - temperature (K).

The Laplace equation is solved first to provide the input for the stress analysis. The thermal load is applied to the structure by utilizing the following condition:

$$T(x, y, z, t)|_L = 30^\circ C \quad (2)$$

where  $L$  denotes a line along which the constant temperature is applied. Two kinds of boundary conditions are assumed. The first condition is applied for convective heat transfer:

$$-(k\nabla T \circ n)|_\Gamma = \alpha(T|_\Gamma - T_a) \quad (3)$$

where  $k$  is thermal conductivity [ $W m^{-1} K^{-1}$ ],  $\alpha$  - convection coefficient ( $W m^{-2} K^{-1}$ ),  $\Gamma$  - boundary surface with convection,  $T|_\Gamma$  - temperature of the surface  $\Gamma$ ,  $T_a$  - ambient temperature and  $n$  - basis vector normal to the surface  $\Gamma$ .

The second condition is applied for isolated surfaces:

$$\nabla T|_\Omega = 0 \quad (4)$$

where  $\Omega$  means an isolated side surface.

The temperature field  $\Delta T$  generated by the thermal analysis is subsequently taken into account in the second step of the sequential analysis by the introduction of the constitutive relationship in the form:

$$\varepsilon = \{C\}^{-1} \{\sigma\} + \{\alpha\} \Delta T \quad (5)$$

where  $\varepsilon$  - strain vector,  $\{C\}$  - elastic stiffness matrix,  $\{\sigma\}$  - stress vector,  $\{\alpha\}$  - thermal expansion coefficient vector,  $\Delta T$  - difference between reference temperature and actual temperature.

No external forces are applied to the structure and two kinds of mechanical boundary conditions are used: free condition and fully suppressed condition.

## NUMERICAL MODEL

For evaluation of the thermal stress field in the layered material, an elementary volume cell corresponding to a piece of the material containing four internal sources of heat (Fig. 2) has been considered. Lateral surfaces are thermally isolated in the thermal analysis. Two kinds of mechanical constraints are considered when performing structural analysis: free boundary conditions and full suppression on lateral surfaces.

Three different materials are analysed: pure glass-epoxy composite material composed of six unidirectional layers  $[0_6]$  (material **M1**), pure carbon-epoxy composite material composed of six unidirectional layers  $[0_6]$  (material **M2**) and combined laminate composed of two carbon-epoxy layers and one glass-epoxy layer in between  $[90/0/90]$  (material **M3**).

Material properties used in numerical analysis for the unidirectional lamina glass-epoxy and carbon-epoxy composite are obtained from the literature [1,3,4,6,7]. They are presented in Tab.1.

Table 1. Material properties of selected unidirectional composites obtained from the literature [1,3,4,6,7].

|  | <b>glass/epoxy</b> | <b>carbon/epoxy</b> |
|--|--------------------|---------------------|
| fiber volume fraction $\nu_f$  | 0.50 [1]           | 0.63 [1]            |
| density $[\text{g}\cdot\text{cm}^{-3}]$                              | 2.00 [1]           | 1.58 [1]            |
| longitudinal modulus $E_L$ [GPa]                                     | 43 [1]             | 142 [1]             |
| transverse modulus $E_T$ [GPa]                                       | 8.9 [1]            | 10.3 [1]            |
| major Poisson's ratio $\nu_{LT}$                                     | 0.27 [1]           | 0.27 [1]            |
| in-plane shear modulus $G_{LT}$                                      | 4.9 [3]            | 4.8 [4]             |
| out-of-plane shear modulus $G_{TT}$                                  | 1.20 [3]           | 4.27 [4]            |
| thermal conductivity $k_L$ [W/m*K]                                   | 0.51 [6]           | 4.50 [7]            |
| thermal conductivity $k_T$ [W/m*K]                                   | 0.345 [6]          | 0.670 [7]           |
| thermal expansion coefficient $\alpha_L$ [ $^{\circ}\text{C}^{-1}$ ] | 5.0e-6 [1]         | -0.9e-6 [1]         |
| thermal expansion coefficient $\alpha_T$ [ $^{\circ}\text{C}^{-1}$ ] | 26.0e-6 [1]        | 27.0e-6 [1]         |

While building the numerical model, the following assumptions have been made:

- the diameter of the conducting wire of the grid, perpendicular to the composite layers, is small compared to the in-plane distance between the wires,
- the in-plane conducting wires of the grid, placed on the outer surfaces of the composite sample, have a small resistivity so that their temperature should rise significantly less, e.g. two orders of magnitude, than the temperature of the perpendicular (through the layers) conducting wires,
- heat is transferred to the environment by convection through the outer surfaces while the boundaries are isolated (this is supposed to model a fragment of a larger composite).

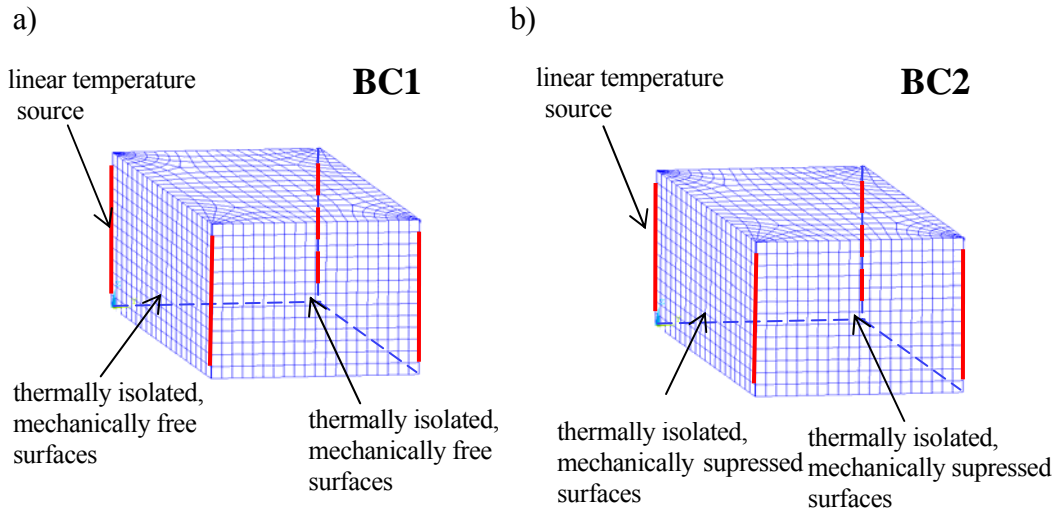


Figure 2. Elementary cell with locations of heat sources and boundary conditions: first case boundary conditions – BC1 a), second case boundary conditions – BC2 b).

The assumed data for the analyzed fragment of the composite are the following: length = 3.2 mm, width = 3.2 mm, height = 2.4 mm for the M1, M2 materials and height = 3.2 mm for the M3 material, applied temperature = 30 °C, ambient temperature = 20 °C, convection coefficient = 10. Higher order 3D solid elements have been used in the FEM analysis.

Table 2. Stresses generated in composite materials.

|                                      | M1<br>BC2<br>[MPa] | M2<br>BC2<br>[MPa] | M3<br>BC1<br>[MPa] | M3<br>BC2<br>[MPa] |
|--------------------------------------|--------------------|--------------------|--------------------|--------------------|
| stress intensity [MPa]               | 14.2               | 17.5               | 7.0                | 22.8               |
| $\sigma_x^{\min.} : \sigma_x^{\max}$ | -14.3 : -8.5       | -17.3 : 3.5        | -2.0:5.3           | -23.1:7.8          |
| $\sigma_y^{\min.} : \sigma_y^{\max}$ | -5.7 : -1.6        | -9.8 : -1.9        | -1.7:2.3           | -12.5:-1.6         |
| $\sigma_z^{\min.} : \sigma_z^{\max}$ | -3.5 : -1.0        | -4.8 : 1.2         | -1.9:2.1           | -5.3:1.2           |

The results of the stress analysis are gathered in Tab. 2. It is worth noting that the stresses obtained for the carbon-epoxy material (M2) are only slightly higher than the stresses for the glass-epoxy material (M1), despite the significant difference in the values of longitudinal moduli of elasticity for these materials (cf. Tab. 1). It seems to be caused by the negative value of the thermal expansion coefficient along fibers for the carbon-epoxy material M2. For the 3-layer material M3, the stresses are concentrated along the interfaces between layers (Fig. 3). The stresses for the multidirectional composite (M3) are higher than the ones for unidirectional material (M1 or M2).

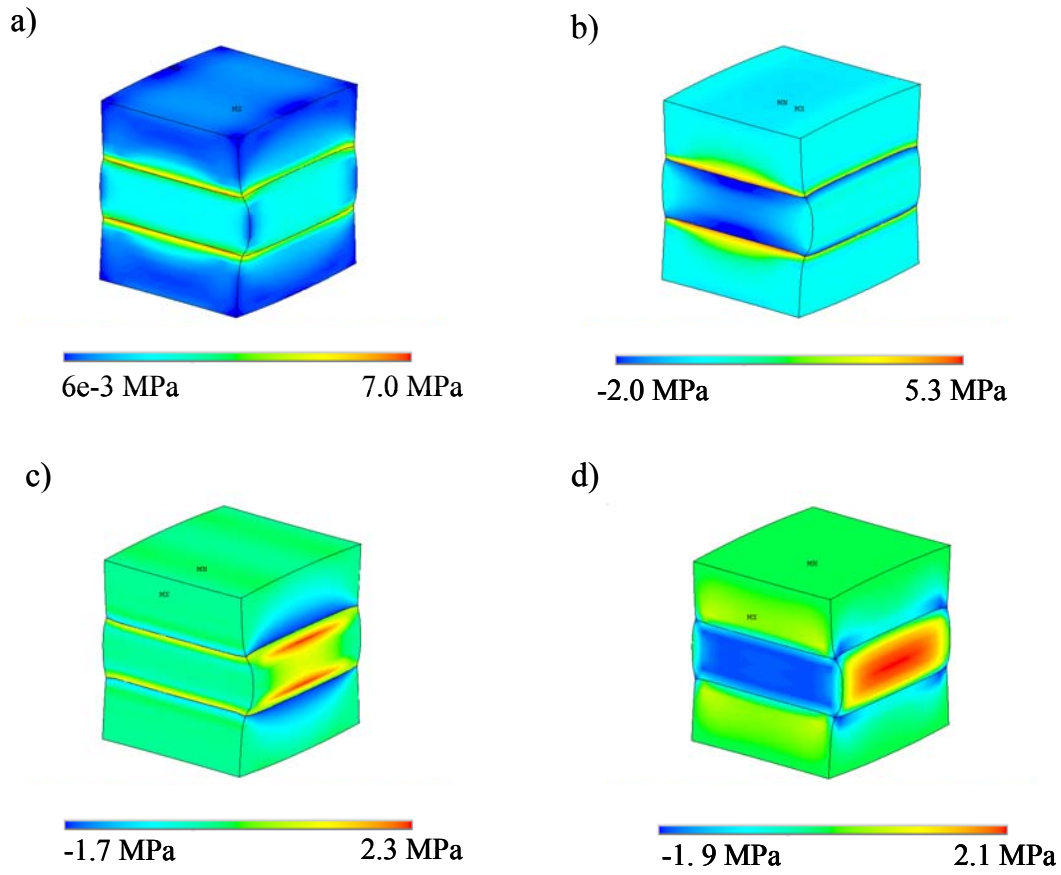


Figure 3. Results for the material M3 with BCI conditions:  $\sigma_x$  a),  $\sigma_y$  b),  $\sigma_z$  c).

## CONCLUSIONS

In this paper, an influence of thermal load on stresses induced in the composite material is investigated. The source of the thermal load in the material is an electrical grid embedded in the composite matrix for SHM purposes. The embedded grid is heated due to the external application of actively controlled electrical current.

It turns out that stresses induced in the material as a result of heating of the embedded grid are moderate compared to the strength capacity of the material. Three types of materials have been considered. The highest stress equal to 23 MPa (compression) has been generated for the multidirectional carbon/glass/carbon composite. Such level of stresses is quite acceptable (just a few per cent of the material strength limit), bearing in mind the potential SHM benefits (cf. [6]) we can have thanks to embedding the electrical grid in the composite.

Future research will be focused on preparation of a detailed model of the composite material including fibers and the surrounding resin rather than using effective values for the homogenized material as stresses may be concentrated on material interfaces.

## ACKNOWLEDGEMENTS

The financial support from the projects “Smart Technologies for Safety Engineering - SMART and SAFE” – TEAM/2008-1/4 Programme – granted by the Foundation for Polish Science and “Modern Material Technologies in Aerospace Industry” – PKAERO – POIG.0101.02-00-015/08 from the EU Structural Funds within the Operational Programme Innovative Economy in Poland is gratefully acknowledged.

## REFERENCES

- [1] H. Altenbach, J. Altenbach, W. Kissing: “Structural Analysis of Laminate and Sandwich Beams and Plates”, Lubelskie Towarzystwo Naukowe, Lublin 2001.
- [2] G. Anagnostopoulos, J. Parthenios, C. Galiotis: ”Thermal stress development in fibrous composites” , Materials Letters 62 (2008) 341-345.
- [3] S. Benli, O. Sayman: “The Effect of Temperature and Thermal Stress on Impact Damage in Laminated Composites”, Mathematical and Computational Applications, Vol. 16, No. 2, pp. 392-403, 2011.
- [4] J. M. Berthelot: “Composite Materials. Mechanical Behavior and Structural Analysis”, Mechanical Engineering Series, Springer-Verlag, 1998.
- [5] J. M. Dulieu-Barton, P. Stanley: „Reproductibility and reliability of the response from four SPATE systems”, Exp. Mech. 37 440-4.
- [6] A. Orłowska, P. Kołakowski, J. Holnicki-Szulc: „Detecting delamination zones in composites by embedded electrical grid and thermographic methods”, Smart Mater. Struct. 20, 105009 (2011).
- [7] C. T. Pan, H. Hocheng: “Prediction of Laser-Induced Thermal Damage of Fiber Mat and Fiber Mat UD Reinforced Polymers”, Journal of Materials Engineering and Performance (1998), 7:751-756.